

点阵多孔金属夹芯板振动特性分析及优化设计*

李拓 江俊

(西安交通大学强度与振动教育部重点实验室, 西安 710049)

摘要 采用空间桁架结构分析的网架结构连续化方法对点阵多孔金属夹芯板的夹芯层桁架进行了连续化处理, 即, 将夹芯层桁架等效为连续介质, 并分别推导了金字塔型、四面体型、kagome型和4杆型点阵多孔金属夹芯板的抗弯刚度和等效剪切刚度。然后, 应用分解刚度法推导了四边简支条件下点阵多孔金属夹芯板的固有振动频率公式, 并与有限元计算结果进行了对比, 表明所得公式具有较高的精度。最后, 研究了夹芯板单胞结构尺寸对固有振动频率的影响, 以夹芯层高度和桁架杆截面尺寸为设计变量, 以第一阶频率最大化为目标对夹芯板进行了优化, 优化后的夹芯板振动频率得到了明显提高。

关键词 点阵多孔金属夹芯板, 振动性能, 网架结构连续化方法, 分解刚度法, 优化设计

引言

点阵多孔金属夹芯板是近年来由 Ashby, Gustafsson, Evan, Wallach & Gibson 等提出的一种新型的多孔金属结构。该结构不仅具有超轻、高比强、高比刚度、高能量吸收^[1-3]等优异的力学性能, 还具有减震、散热、吸声、电磁屏蔽、渗透性强等功能作用^[4-9]。其兼具结构和功能的特性, 在航空航天、机械、铁路、汽车、建筑、能源等领域有广泛的应用前景。另外, 针对其他类型夹芯板的振动特性和非线性响应也开展了工作^[17, 18]。

目前, 已经提出多种拓扑构型点阵多孔金属夹芯板, 包括金字塔型^[2], 四面体型^[8, 10], kagome型^[11], 4杆型^[12]等。近年来, 国内外学者在点阵多孔金属夹芯板的制备^[13-15]、力学性能^[1-3]、优化设计^[8, 12, 16]和多功能应用^[4-7]等方面开展了众多研究工作。

点阵多孔金属夹芯板在航天、航空、船舶、汽车、高速列车等应用领域复杂的振动环境要求下, 有必要对该结构的振动特性进行详细研究, 而该方面的研究十分有限。本文采用网架结构连续化方法^[19]将点阵多孔金属夹芯板夹芯层桁架等效为连续介质, 采用经典的 Reissner 夹层板分析理论^[20]对等效后的夹层板进行分析, 分别推导了金字塔型、四面体型、kagome型和4杆型点阵多孔金属夹

芯板的抗弯刚度和等效剪切刚度, 并应用分解刚度法得到了四边简支条件下这四种典型构型点阵多孔金属夹芯板固有振动频率理论公式。最后, 以夹芯层高度和夹芯桁架杆截面尺寸为设计变量, 以固有振动第一阶频率最大化为目标对四种典型构型点阵多孔金属夹芯板进行了优化分析。

1 等效思想和基本假定

点阵多孔金属夹芯板夹芯层桁架为平板型网架结构, 从结构整体、外形尺寸、周期性排布等宏观角度来看, 可用一块连续介质平板来等效。本文采用网架结构连续化方法将夹芯层桁架等效为连续介质, 如图1所示。

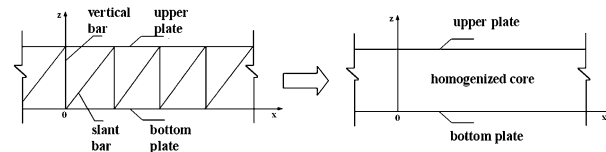


图1 点阵多孔金属夹芯板夹芯层桁架等效示意图

Fig. 1 Schematic plot of the homogenization of the truss-cored metal sandwich plate

Reissner 夹层板分析理论在经典弹性薄板理论基础上考虑了夹芯层的剪应变, 有如下基本假定:

(i) 网架稠密, 一般要求网架结构在短跨方向的网格数要大于或等于 5。

(ii) 假定夹层板的上下面板不能承受横向剪力,为平面应力状态.

(iii) 把夹芯桁架的斜腹杆与竖腹杆等效为连续介质的夹芯层,厚度为夹芯高度 h_c , 夹芯层只承受剪力,不承受轴向力. 即夹芯层只有横向剪切刚度,忽略平面刚度.

(iv) 垂直板面的直线段在变形后仍为直线段,并在 xz , yz 平面内分别转了一个角度 ϕ_x , ϕ_y , 但不再垂直于挠曲后的板面. $\phi_x = \frac{\partial w}{\partial x} - \gamma_x$, $\phi_y = \frac{\partial w}{\partial y} - \gamma_y$ 其中 γ_x , γ_y 为剪切角,如图 2 所示.

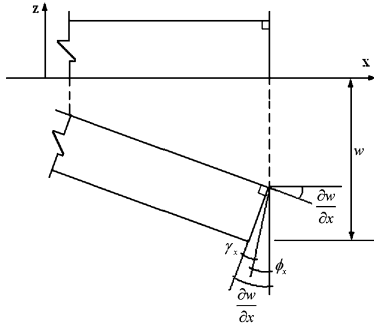


图 2 等效夹层板板剪切角示意图

Fig. 2 Schematic plot of the shear angles of homogenized sandwich plate

2 抗弯刚度和等效剪切刚度

平面应力状态下上、下面板的物理方程为

$$\begin{Bmatrix} \sigma_x \\ \sigma_y \\ \sigma_{xy} \end{Bmatrix} = \frac{Et}{1-\mu^2} \begin{Bmatrix} 1 & v & 0 \\ v & 1 & 0 \\ 0 & 0 & \frac{1-v}{2} \end{Bmatrix} \begin{Bmatrix} \varepsilon_x \\ \varepsilon_y \\ \varepsilon_{xy} \end{Bmatrix} \quad (1)$$

令 $B^u = B^d = \frac{Et}{1-\mu^2} \begin{Bmatrix} 1 & v & 0 \\ v & 1 & 0 \\ 0 & 0 & \frac{1-v}{2} \end{Bmatrix}$, 分别为上下

面板的薄膜刚度矩阵, 整块夹芯板的薄膜刚度矩阵 $B = B^u + B^d$, 夹芯板的抗弯刚度矩阵^[20]为

$$D = \frac{1}{4} h^2 B = D^* \begin{Bmatrix} 1 & v & 0 \\ v & 1 & 0 \\ 0 & 0 & \frac{1}{2}(1-v) \end{Bmatrix} \quad (2)$$

其中: $D^* = \frac{Eh^2 t}{2(1-v^2)}$

3 夹芯层等效剪切刚度

采用文献[19]提出的网架结构连续化方法对

夹芯层桁架分析, 分别得到四种典型构型点阵多孔金属夹芯板等效剪切刚度. 单胞结构尺寸见图 3.

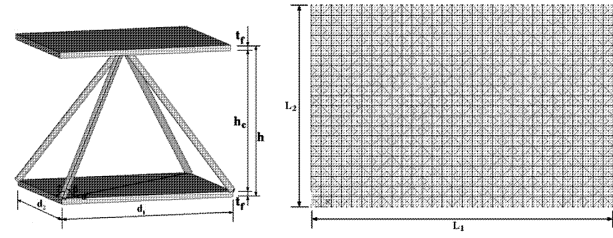


图 3 金字塔型点阵多孔金属夹芯板单胞及有限元模型

Fig. 3 A unit cell of pyramidal truss-cored metal sandwich plate and the mesh of the plate in finite element method

(a) 金字塔型点阵多孔金属夹芯板等效剪切刚度

$$\alpha_1 = \frac{\pi}{4}, \alpha_2 = \frac{\pi}{4}, d_1 = d_2 = d$$

$$\bar{\Delta}_1 = \bar{\Delta}_2 = \frac{\sqrt{2}}{2}d, C_1 = C_2 = EA_c \sin^2 \beta \cos \beta \quad (3)$$

$$\text{则 } C_{11} = C_{22} = \frac{\sqrt{2}EA_c \sin^2 \beta \cos \beta}{d}, C_{12} = C_{21} = 0$$

(b) 四面体型点阵多孔金属夹芯板等效剪切刚度

$$\alpha_1 = \frac{\pi}{2}, \alpha_2 = -\frac{\pi}{6}, \alpha_3 = \frac{\pi}{6}, d_1 = d_2 = d$$

$$\bar{\Delta}_1 = d, \bar{\Delta}_2 = \bar{\Delta}_3 = \frac{3}{4}d, C_1 = \frac{2}{3}EA_c \sin^2 \beta \cos \beta$$

$$C_2 = C_3 = \frac{1}{2}EA_c \sin^2 \beta \cos \beta \quad (4)$$

$$\text{则 } C_{11} = C_{22} = \frac{EA_c \sin^2 \beta \cos \beta}{d}, C_{12} = C_{21} = 0$$

(c) kagome 型点阵多孔金属夹芯板等效剪切刚度

$$\alpha_1 = 0, \alpha_2 = \frac{\pi}{3}, \alpha_3 = -\frac{\pi}{2}, d_1 = d, d_2 = \frac{\sqrt{3}}{2}d,$$

$$\bar{\Delta}_1 = \frac{\sqrt{3}}{2}d, \bar{\Delta}_2 = \bar{\Delta}_3 = \sqrt{3}d, C_1 = \frac{1}{2}EA_c \sin^2 \beta \cos \beta$$

$$C_2 = C_3 = \frac{1}{4}EA_c \sin^2 \beta \cos \beta \quad (5)$$

$$\text{则有 } C_{11} = C_{22} = \frac{\sqrt{3}EA_c \sin^2 \beta \cos \beta}{8d}, C_{12} = C_{21} = 0$$

(d) 四杆型点阵多孔金属夹芯板等效剪切刚度

$$\alpha_1 = \frac{\pi}{4}, \alpha_2 = -\frac{\pi}{4}, d_1 = d, d_2 = \frac{\sqrt{3}}{2}d,$$

$$\bar{\Delta}_1 = \bar{\Delta}_2 = \sqrt{2}d, C_1 = C_2 = \frac{1}{4}EA_c \sin^2 \beta \cos \beta \quad (6)$$

$$\text{则有 } C_{11} = C_{22} = \frac{\sqrt{2}EA_c \sin^2 \beta \cos \beta}{8d}, C_{12} = C_{21} = 0$$

4 分解刚度法进行固有振动分析

在惯性力作用下的夹芯板产生竖向振动,夹芯板的动能为

$$W = \frac{1}{2} \iint_{\Omega} \rho^* \omega_{mn}^2 w^2 dx dy = \frac{1}{2} \rho^* \omega_{mn}^2 \iint_{\Omega} w^2 dx dy \quad (7)$$

其中, $\rho^* = h_c \rho_c + 2t \rho_f$ 为夹芯板单位面积的质量, ρ_f 为面板的密度, ρ_c 为夹芯层的等效密度, ω_{mn} 为夹芯板的无阻尼自由振动圆频率.

夹芯板的总势能为

$$\begin{aligned} \Pi &= \frac{1}{2} \iint_{\Omega} [D_{11} (\frac{\partial \phi_x}{\partial x})^2 + D_{22} (\frac{\partial \phi_y}{\partial y})^2 + D_{33} (\frac{\partial \phi_x}{\partial y} \\ &+ \frac{\partial \phi_y}{\partial x})^2 + 2D_{12} \frac{\partial \phi_x}{\partial x} \frac{\partial \phi_y}{\partial y} + C_{11} (\frac{\partial w}{\partial x} - \phi_x)^2 + C_{22} (\frac{\partial w}{\partial y} \\ &- \phi_y)^2 + 2C_{12} (\frac{\partial w}{\partial x} - \phi_x) (\frac{\partial w}{\partial y} - \phi_y) - \rho^* \omega_{mn}^2 w^2] dx dy \end{aligned} \quad (8)$$

按照分解刚度的思想,令 w_b 为 $C \rightarrow \infty$ 而 D 保持不变时的挠度, w_s 为 $D \rightarrow \infty$ 而 C 保持不变时的挠度,则三个广义位移可表达为

$$\begin{cases} w = w_b + w_s \\ \phi_x = \frac{\partial w_b}{\partial x} \\ \phi_y = \frac{\partial w_b}{\partial y} \end{cases} \quad (9)$$

其中: w_b, w_s 分别为夹层板的弯曲挠度和剪切挠度.

根据式(9)可将式(8)分解为

$$\Pi = \Pi_b + \Pi_s \quad (10)$$

其中:

$$\begin{aligned} \Pi_b &= \frac{1}{2} \iint_{\Omega} [D_{11} (\frac{\partial^2 w_b}{\partial x^2})^2 + D_{22} (\frac{\partial^2 w_b}{\partial y^2})^2 + \\ &4D_{33} (\frac{\partial^2 w_b}{\partial x \partial y})^2 + 2D_{12} \frac{\partial^2 w_b}{\partial x^2} \frac{\partial^2 w_b}{\partial y^2} - \rho^* \omega_{bmn}^2 w_b^2] dx dy \\ \Pi_s &= \frac{1}{2} \iint_{\Omega} [C_{11} (\frac{\partial w_s}{\partial x})^2 + C_{22} (\frac{\partial w_s}{\partial y})^2 + 2C_{12} \frac{\partial w_s}{\partial x} \\ &\frac{\partial w_s}{\partial y} - \rho^* \omega_{smn}^2 w_s^2] dx dy \end{aligned}$$

取振型函数为:

$$\begin{cases} w_b = \sum_m \sum_n A_{mn}^b \sin(\frac{m\pi x}{L_1}) \sin(\frac{n\pi y}{L_2}) \\ w_s = \sum_m \sum_n A_{mn}^s \cos(\frac{m\pi x}{L_1}) \cos(\frac{n\pi y}{L_2}) \end{cases} \quad (11)$$

将式(11)代入式(10)进行积分,由势能驻值原理

$$\frac{\partial \Pi_b}{\partial A_{mn}^b} = 0, \frac{\partial \Pi_s}{\partial A_{mn}^s} = 0$$

得:

$$\begin{cases} \omega_{bmn}^2 = \frac{\pi^4 (m^4 D_{11} + 2m^2 n^2 \lambda D_{12} + n^4 \lambda^4 D_{22} + 4m^2 n^2 \lambda^2 D_{33})}{L_1^4 \rho^*} \\ \omega_{smn}^2 = \frac{\pi^2 (m^2 C_{11} + n^2 \lambda^2 C_{22} - 2\lambda C_{12})}{L_1^2 \rho^*} \end{cases} \quad (12)$$

式中, $\lambda = L_2/L_1$, 夹芯板的自振频率为

$$\omega_{mn} = \sqrt{\frac{\omega_{bmn}}{1 + \left(\frac{\omega_{bmn}}{\omega_{smn}}\right)}} \quad (13)$$

将式(2)、式(12)式代入(13), 得

$$\omega_{mn} = \sqrt{\frac{D^* p^2}{\rho^* (1 + \frac{D^2}{C^2} p)}} \quad (14)$$

其中: $p = \frac{\pi^2}{L_1^2} (m^2 + n^2 \lambda^2)$, $m = 1, 2, 3 \dots$, $n = 1, 2, 3 \dots$

$\dots, \lambda = L_1/L_2$

5 分解刚度法与有限元计算结果对比

点阵多孔金属夹芯板的上下面板都采用不锈钢材料, 弹性模量 $E = 200 GPa$, 密度 $\rho = 8000 kg/m^3$, 泊松比 $\nu = 0.3$, 上下面板的厚度 $t_f = 1.0 mm$, 夹芯层高度 $h_c = 30 mm$, 夹芯桁架杆截面尺寸 $b \times b = 1.5 mm \times 1.5 mm$, 单胞长度和宽度 $d_1 = d_2 = 42.2 mm$, 夹芯板长 $L_1 = 45d_1$, 宽 $L_2 = 30d_2$, 其四边简支.

有限元模拟采用商用软件 Ansys 进行计算. 上下面板采用 shell91 单元, 上面板节点取在板下方, 厚度向上偏置, 下面板节点取在板上方, 厚度向下偏置, 腹杆采用 beam4 单元; 桁架杆与面板连接结点所有自由度耦合. 夹芯板四边简支. 模态分析选用子空间迭代法.

从表 1-4 可以看出, 采用分解刚度法所得固有振动频率公式计算的四种典型构型点阵多孔材料夹芯板的前 6 阶频率, 与有限元计算结果吻合很好, 误差在 7% 以内. 表明分解刚度法所得固有振动频率公式可以对点阵多孔材料夹芯板的低阶固有振动频率进行很好的预测, 且抗弯度和等效剪切刚度的推导简单易行.

表1 金字塔型点阵多孔金属夹芯板分解刚度法
与有限元计算固有振动频率结果(单位Hz)

Table 1 Results of the natural frequencies of a pyramidal truss-cored metal sandwich plate by MSR and FEM

mode	1	2	3	4	5	6
FEM	101.47	179.47	266.53	292.40	326.10	415.90
MSR	101.72	183.36	273.36	300.99	337.99	434.71
Error (%)	0.25	2.17	2.56	2.94	3.65	4.52

表2 四面体型点阵多孔金属夹芯板分解刚度法
与有限元计算固有振动频率结果(单位Hz)

Table 2 Results of the natural frequencies of a tetragonal truss-cored metal sandwich plate by MSR and FEM

mode	1	2	3	4	5	6
FEM	120.26	192.98	296.41	314.60	364.81	415.35
MSR	120.94	195.92	301.79	320.82	374.56	424.07
Error (%)	0.57	1.52	1.81	1.98	2.67	2.10

表3 kagomé型点阵多孔金属夹芯板分解刚度法
与有限元计算固有振动频率结果(单位Hz)

Table 3 Results of the natural frequencies of a kagomé truss-cored metal sandwich plate by MSR and FEM

mode	1	2	3	4	5	6
FEM	74.01	110.91	146.25	157.37	168.66	201.67
MSR	75.61	107.04	146.17	152.87	171.44	188.24
Error (%)	2.17	-3.49	-0.05	-2.86	1.65	-6.66

表4 4杆型点阵多孔金属夹芯板分解刚度法
与有限元计算所得固有振动频率结果(单位Hz)

Table 4 Results of the natural frequencies of a 4-rod truss-cored metal sandwich plate by MSR and FEM

mode	1	2	3	4	5	6
FEM	62.41	94.51	124.55	133.23	144.38	172.75
MSR	63.22	95.34	125.34	133.94	145.16	173.38
Error (%)	1.30	0.88	0.63	0.53	0.54	0.37

6 优化设计

计算结构的低阶固有频率,可以有效防止结构的外部激励与其固有振动频率相近,从而导致结构因发生共振而破坏.因此,尽量提高结构固有振动第一阶频率是防止发生结构共振的有效途径之一.

从式(14)可知,影响固有振动频率的主要是抗弯刚度和剪切刚度,随着抗弯刚度 D^* 的增大,固有频率会增大,随着剪切刚度的增大,固有频率也

增大.但从式(2)和式(3)-(6)可以看出,点阵多孔金属夹芯板单胞结构尺寸的变化会同时引起抗弯刚度和剪切刚度的变化.因此在边界条件不变,使用同种材料的情况下,单胞结构尺寸是影响夹芯板固有振动频率的重要参数,即 $\omega(h_c, b, d, t_f, \lambda)$. 分析式(2)和式(3)-(6),得知夹芯层高度 h_c 对抗弯刚度有最大的影响,桁架杆截面尺寸 b 对剪切刚度有最大的影响.

本文以夹芯层高度 h_c 和桁架杆截面尺寸 b 为设计变量,以夹芯板固有振动第一阶频率最大化为目标进行了优化设计.

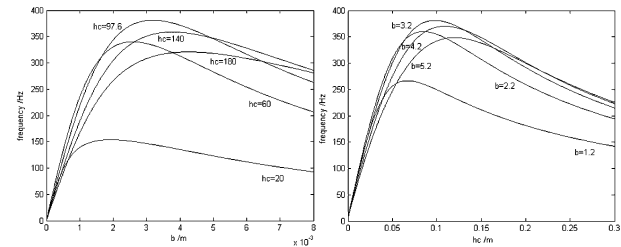


图4 第一阶固有振动频率与 h_c 和 b 的变化关系

Fig. 4 The influence of h_c and b on the first natural frequency

根据式(14),用matlab编程进行优化分析,点阵多孔金属夹芯板各结构参数及 h_c 和 b 的初始值与上文所述模型相同.

表5给出了各构型点阵多孔金属夹芯板固有振动第一阶频率优化后的最大值及取最大值对应的 h_c 和 b 的取值.对于金字塔型点阵多孔金属夹芯板,当 $b = 3.2\text{mm}$, $h_c = 97.6\text{mm}$ 时,固有振动第一阶频率有最大值 $\omega_{1,\max} = 381.22\text{Hz}$,相对于其未优化前的固有振动第一阶频率 $\omega_1 = 101.22\text{Hz}$ 有了很显著的提高.分析第一阶固有振动频率与 h_c 和 b 的变化关系(图4),还可以得出如下结论:

- (a) 当 h_c 不变时,第一阶频率随 b 呈抛物线变化,先增加到峰值,然后减小;
- (b) 当 $h_c < h_{c,max}$ 时,随着 h_c 的增大,峰值增大,当 $h_c > h_{c,max}$ 时,随着 h_c 的增大,峰值减小;
- (c) 随着 h_c 的增大,要使得第一阶固有振动频率取峰值的 b 的取值增大;
- (d) 当 b 不变时,第一阶固有振动频率随 h_c 的呈抛物线变化,先增加到峰值,然后减小;
- (e) 当 $b < b_{max}$ 时,随着 b 的增大,峰值增大,当 $b > b_{max}$ 时,随着 b 的增大,峰值减小;
- (f) 随着 b 的增大,要使得第一阶频率取峰值的 h_c

的取值增大.

表5 点阵多孔金属夹芯板优化后第一阶固有振动频率

Table 5 Optimized first natural frequencies of
the truss-cored metal sandwich plates

Truss type	b/mm	h_c/mm	$\omega_{1,\max}/\text{Hz}$	ω_1/Hz
Pyramid	3.20	97.60	381.22	101.47
Tetrahedral	3.28	101.00	223.13	120.26
Kagomé	5.36	95.00	179.99	74.01
4-rod truss	4.28	53.60	94.91	62.41

7 结论

本文从等效思想出发,采用空间网架结构连续化方法将点阵多孔金属夹芯板桁架等效为连续介质,根据 Reissner 夹层板分析理论分析等效后的夹芯板. 分别推导了金字塔型、四面体型、kagome 型和 4 杆型点阵多孔金属夹芯板的抗弯刚度和等效剪切刚度,利用分解刚度法推导得到四边简支条件下四种典型构型点阵多孔金属夹芯板的固有振动频率公式. 等效抗弯度和等效剪切刚度的推导简单易行,且分解刚度法所得固有振动频率公式计算频率结果与有限元计算计算结果吻合很好,对点阵多孔材料夹芯板的低阶固有振动频率可进行很好的预测.

点阵多孔金属夹芯板的振动性能与单胞结构尺寸有密切关系,对固有振动频率公式的分析认为夹芯层高度 h_c 和桁架杆的截面尺寸对振动性能的影响最大. 随后,以这两个参数为设计变量,以夹芯板固有振动第一阶频率最大为目标进行了优化分析. 优化后的夹芯板振动频率明显得到了提高,且 h_c 和的取值在合理范围内. 这对应用于航天、航空、船舶、汽车、高速列车等领域的点阵多孔金属夹芯板在设计时考虑防止共振,提高低阶频率具有很好的参考价值.

参 考 文 献

- Evans AG, Hutchinson JW, Fleck NA, et al. The topological design of multifunctional cellular metals. *Progress in Materials Science*, 2001, 46 (3-4) : 309 ~ 327
- Wallach JC, Gibson LJ. Mechanical behavior of a three-dimensional truss material. *International Journal of Solids and Structures*, 2001, 38 (40-41) : 7181 ~ 7196
- Hutchinson JW, Xue Z. Metal sandwich plates optimized for pressure impulses. *International Journal of Mechanical Sciences*, 2005, 47 (4-5) : 545 ~ 569
- Tian J, Kim T, Lu TJ, et al. The effects of topology upon fluid-flow and heat-transfer within cellular copper structures. *International Journal of Heat and Mass Transfer*, 2004, 47 (14-16) : 3171 ~ 3186
- Kim T, Zhao CY, Lu TJ, et al. Convective heat dissipation with lattice-frame materials. *Mechanics of Materials*, 2004, 36 (8) : 767 ~ 780
- Ruzzene M. Vibration and sound radiation of sandwich beams with honeycomb truss core. *Journal of Sound and Vibration*, 2004, 277 (4-5) : 741 ~ 763
- Kawahara S, Ueda M, Maegawa S, et al. Magnetization and NMR studies of the spin antiferromagnet on the kagome lattice. *Journal of Magnetism and Magnetic Materials*, 2004, 272-276 Supplement 1: E999 ~ E1000
- Wicks N, Hutchinson JW. Optimal truss plates. *International Journal of Solids and Structures*, 2001, 38 (30-31) : 5165 ~ 5183
- Wang J, Evans AG, Dharmasena K, et al. On the performance of truss panels with Kagome cores. *International Journal of Solids and Structures*, 2003, 40 (25) : 6981 ~ 6988
- Deshpande VS, Fleck NA. Collapse of truss core sandwich beams in 3-point bending. *International Journal of Solids and Structures*, 2001, 38 (36-37) : 6275 ~ 6305
- Hyun S, Karlsson AM, Torquato S, et al. Simulated properties of Kagome and tetragonal truss core panels. *International Journal of Solids and Structures*, 2003, 40 (25) : 6989 ~ 6998
- Liu T, Deng ZC, Lu TJ. Design optimization of truss-cored sandwiches with homogenization. *International Journal of Solids and Structures*, 2006, 43 (25-26) : 7891 ~ 7918
- Deshpande VS, Fleck NA, Ashby MF. Effective properties of the octet-truss lattice material. *Journal of the Mechanics and Physics of Solids*, 2001, 49 (8) : 1747 ~ 1769
- Wadley HNG, Fleck NA, Evans AG. Fabrication and structural performance of periodic cellular metal sandwich structures. *Composites Science and Technology*, 2003, 63 (16) : 2331 ~ 2343
- Brittain ST, Brittain ST, Sugimura Y, et al. Fabrication and mechanical performance of a mesoscale space-filling truss system. *Microelectromechanical Systems, Journal of*, 2001, 10 (1) : 113 ~ 120
- Liu J-S, Lu TJ. Multi-objective and multi-loading optimization of ultralightweight truss materials. *International Journal*

- of Solids and Structures*, 2004, 41 (3-4) : 619 ~ 635
- 17 孙佳, 张伟, 陈丽华, 姚明辉. 蜂窝夹层板的非线性动力学研究. 动力学与控制学报, 2008, 6(2) : 150 ~ 155 (Sun Jia, Zhang Wei, Chen Lihua, Yao Minghui. Nonlinear dynamics of the honeycomb sandwich plates. *Journal of Dynamics and Control*, 2008, 6(2) : 150 ~ 155 (in Chinese))
- 18 胡宁宁, 张永发. 变厚度智能硬夹心板振动分析. 动力学与控制学报, 2003, 1(1) : 70 ~ 73 (Hu Ningning, Zhang Yongfa. Vibration analysis of smart changed hard sandwich plate. *Journal of Dynamics and Control*, 2003, 1(1) : 70 ~ 73 (in Chinese))
- 19 董石麟, 钱若军. 空间网格结构分析理论与计算方法.

北京: 中国建筑工业出版社, 2000 (Dong Shilin, Qian Ruojun. Analysis theory and computation methods for space grid structure. Beijing: Chinese Architecture Industrial Publisher, 2000 (in Chinese))

- 20 中国科学院北京力学研究所固体力学研究室板壳组. 夹层板壳的弯曲稳定和振动. 北京: 科学出版社, 1977 (Plate and Shell Group, Solid Mechanics Division, Beijing Mechanics Institute. Chinese Science Academy, Bending Stability and Vibration of Sandwich Plates and Shells. Beijing: Science and Technology Publisher, 1977 (in Chinese))

VIBRATION CHARACTERISTICS AND OPTIMIZATION OF TRUSS-CORED METAL SANDWICH PLATES^{*}

Li Tuo Jiang Jun

(MOE Key Laboratory of Strength and Vibration, Xi'an Jiaotong University, Xi'an 710049, China)

Abstract The space grid homogenization theory used in space grids design was adopted to homogenize the truss-cored metal sandwich plates. The bending stiffness and equivalent shear stiffness of the homogenized plates were obtained by using Reissner sandwich theory and the space grid homogenization method respectively. The formulae of the natural frequencies of four typical truss-cored metal sandwich plates were then derived by using the Method of Split Rigidities (MSR). The frequencies of truss-cored metal sandwich plates obtained by the formulae are in good agreement with those by finite element method. Moreover, the influence of structure parameter of the unit cell on the natural frequencies was analyzed. Optimization with the goal of a maximal first natural frequency was performed by optimizing the height of truss core and the cross-sectional area of the truss. The truss-cored metal sandwich plates after optimization have a much higher first frequency compared with the original design.

Key words truss-cored metal sandwich plate, vibration characteristics, homogenization, Method of Split Rigidities, optimization